Published in Journal of the Optical Society of America A 22, issue 1, 109-116, 2005
which should be used for any reference to this work


# Calculation of the torque on dielectric elliptical cylinders

**Carsten Rockstuhl and Hans Peter Herzig**

*University of Neuchâtel, Institute of Microtechnology, Rue Breguet 2, CH-2000 Neuchâtel, Switzerland*

We present our investigation of the torque exerted on dielectric elliptical cylinders by highly focused laser beams. The calculations are performed with rigorous diffraction theory, and the size-dependent torque is analyzed as a function of the axis ratio. It is found that highly elongated particles will experience a reversal of the torque for a radius that is approximately one third of the wavelength. This effect is attributed to interference effects inside the structure due to multiple reflections of the incoming wave. The evolution from a perfectly sinusoidal angular dependence of the torque to a more complicated pattern for increasing particle size is presented in detail.

## 1. INTRODUCTION

Since the pioneering work of Ashkin in the 1970s,[1–3] the optical force and torque exerted on particles by optical wave fields has become a subject of intensive research because of the fascinating physics and interesting potential applications. The force on dielectric particles basically leads to an acceleration of the particles in the propagation direction of the beam and to an attraction toward the optical axis if the particles are sufficiently large compared to the wavelength.[4] Numerical computation of the behavior in this size regime can be done efficiently with a technique based on geometrical optics.[5] A characterization of the force on particles that are much smaller than the wavelength can be performed with a dipole approximation.[6] Within the approach, the entire force is decomposed into a scattering and a gradient component. The scattering component points in the propagation direction of the incoming beam and the gradient force in the direction of the gradient of the square of the absolute value of the electric field. For highly focused laser beams, this component of the force will point correspondingly to the waist of the beam. If the $z$ component of the gradient force equals the scattering force, a stable trapping of particles in three dimensions is possible. Such an optical tweezer can be used for applications such as scanning near-field optical microscopy, in which a trapped particle serves as a highly localized near-field probe,[7] or for photonic force microscopy.[8]

Another interesting possibility is to rotate the particles by exploiting the torque applied to them, using various mechanisms.[9] One approach is to use directly the properties of the illuminating wave field, such as the orbital angular momentum of the beam[10] (associated with helical phase fronts) or its spin angular momentum[11] (associated with circular polarization).

Another mechanism for the rotation of a particle is its nonspherical geometry, causing an alignment of the particle relative to the laser beam, as was demonstrated in some recent experiments.[12–14] The fascinating exploitations of the torque exerted on microparticles in applications such as the construction of micromachines driven by light[15,16] or as a possible microrheometer[17] motivated some researchers to analyze the torsion of particles not only experimentally but also theoretically.[5,12,18] However, because of the complex calculations required, only the specific experimental configurations were normally treated numerically, in order to compare theory and experiment. In most cases, particles with a size significantly smaller than the optical wavelength have been analyzed, meaning that effects that appear if the size of the particles is comparable to the wavelength were not discussed.

In this paper we present a detailed analysis of the torque on dielectric cylinders with an elliptical cross section for different size domains. The structures are essentially two dimensional, and thus invariant in the third dimension. We analyzed such a geometry because the necessary solution of the three-dimensional scattering problem would exceed a reasonable computation time, as well as memory size. However, the main effects that appear in a two-dimensional simulation will be qualitatively comparable to the three-dimensional case.

The particles positioned in the $x-z$ plane are illuminated with a highly focused Gaussian beam. As given by the dipole model, for very small elliptical particles the exerted torque shows a perfectly sinusoidal dependence on the angle between the optical axis and the axis of the particle. In this size domain the torque has a different sign for the different polarizations. For TM polarization (the magnetic field oscillates parallel to the infinite cylinder axis in the $y$ direction) the particles will be aligned along the major axis, whereas for TE polarization (the electric field oscillates parallel to the infinite cylinder axis in the $y$ direction) they will be aligned along the minor axis. To increase the size, an inversion of the sign appears for highly elongated particles. For particles having a size comparable to the wavelength, the torque response becomes quite complex, and different angles exist for which

the particles are rotationally stably trapped, having zero net torque.

## 2. COMPUTATIONAL PROCEDURE

The computational procedure basically consists of two steps. First, the complex field distribution along the surface of the particle is calculated by using rigorous diffraction theory. In the special case of a sphere in three dimensions or a circular cylinder in two dimensions, Mie theory can be used as a quasi-analytical solution for the problem.[19] For deviating geometries Nieminen *et al.* used the $T$-matrix method to calculate the torque on the particles.[20] We use the multiple multipole method for the solution of the diffraction process,[21] which is comparable to the T-matrix method. The multiple multipole method was used by Novotny and co-workers to model the near-field interaction of very small particles with the tip of a scanning near-field microscope that was used as an optical tweezer on a nanometric-length scale.[22] They also presented a calculation of the torque on a very small elliptical particle. However, these calculations were done only for a single specific example.

In the multiple multipole method the field in regions with a homogeneous dielectric constant is expanded in modes, which are an analytical solution of the wave equation. The amplitude of the modes are optimized in a least-squares sense such that the boundary conditions (the continuity of the field and its derivative across the boundary between two regions with a homogeneous dielectric constant) are fulfilled. In the present study we used Hankel functions of the first order with five expansion terms as the basis for the mode expansion and 75 multipoles.[23] The surface was sampled with 500 points. The multipoles that describe the field inside the particles are positioned somewhat behind the boundary, in the surrounding medium, and the multipoles describing the scattered field are positioned within the particle. This is done to avoid the singularities of the field associated with the origins of the multipoles.

The illuminating beam was decomposed into 41 plane waves. This allows the calculation of the field across the particle at an arbitrary point in space by a subsequent superposition of the plane-wave response, multiplied by the amplitude of the Fourier transform of the illuminating wave field. This leads to a reduction in computation time and allows us to analyze the force and torque on particles for different illuminating wave fields. If the particle is positioned at a point $(x, z)$ relative to the center of the waist of the beam, the complex amplitude of the $m$th-order illumination plane wave is given by

$$A_m = \frac{\exp\left[-i\left(\frac{2\pi}{\lambda} - m\frac{2\pi}{\lambda}z\right)^{1/2}\right]}{\Lambda} \times \int_{-\Lambda/2}^{\Lambda/2} a_{\mathrm{Inc}}(x)\exp\left(-im\frac{2\pi}{\Lambda}x\right)^{1/2} \mathrm{d}x, \qquad (1)$$

with $a_{\mathrm{Inc}}(x)$ being the amplitude distribution of the incident wave field in the waist. The discretization will introduce a period of $\Lambda$ in the illuminating beam. Usually we use a period of $20\lambda$. This number was chosen to be sufficiently high such that interference of the illumination beam between adjacent periods is negligible. As the illumination field we use a Gaussian beam given by

$$a_{\mathrm{Inc}}(x) = E_0 \exp\left[-\left(\frac{x}{\omega}\right)^2\right], \qquad (2)$$

with $E_0$ being the beam amplitude. The amplitude was chosen to be 6.9 V/m, which corresponds to the amplitude of a three-dimensional beam with a power of 100 mW. $\omega$ is the waist of the beam. Unless otherwise stated, we have chosen the beam waist to be equal to the wavelength.

In the second step of the calculation, once the field across the surface of the particle is known, we then apply Maxwell's stress tensor $\tilde{T}$ to calculate the force that acts on the particle by integrating over the surface of the particle[24]:

$$\mathbf{F} = \oint (\tilde{T} \cdot \mathbf{n})\mathrm{d}A, \qquad (3)$$

where $\mathbf{n}$ is the unit vector normal to the surface. At optical frequencies, only the time average of the electromagnetic force $\langle \mathbf{F} \rangle$ is observed. For a particle embedded in an isotropic medium, the force is calculated as[25]

$$\begin{aligned}\langle \mathbf{F} \rangle &= \left\langle \oint (\tilde{T} \cdot \mathbf{n})\mathrm{d}A \right\rangle \\ &= \int_S \left\{ \frac{\epsilon}{2}\mathrm{Re}[(\mathbf{E}\cdot\mathbf{n})\mathbf{E}^*] - \frac{\epsilon}{4}(\mathbf{E}\cdot\mathbf{E}^*)\mathbf{n} \right. \\ &\quad \left. + \frac{\mu}{2}\mathrm{Re}[(\mathbf{H}\cdot\mathbf{n})\mathbf{H}^*] - \frac{\mu}{4}(\mathbf{H}\cdot\mathbf{H}^*)\mathbf{n} \right\} \mathrm{d}l', \qquad (4)\end{aligned}$$

with $\epsilon$ being the dielectric constant of the surrounding medium, $\mu$ its permittivity, and $dl'$ the length of a line segment of the surface. The net radiation torque on the particle is calculated subsequently by[24]

$$\langle \tau \rangle = \left\langle \oint \mathbf{r} \times (\tilde{T} \cdot \mathbf{n})\mathrm{d}A \right\rangle, \qquad (5)$$

where $\mathbf{r}$ is the vector between the element of integration on the surface and a reference point within the particle that is assumed to be the point around which the particle rotates. In the calculations we have used the center of the particle as the reference point. However, the exact point is not important as the calculated torque will be the same, regardless of the choice of position.

The particles used in the simulations have an elliptical cross section. The size of the major axis with radius $r_1$ is the reference radius $r_{\mathrm{Ref}}$ multiplied by three different factors: $\sqrt{4}$, $\sqrt{3}$, and $\sqrt{2}$. The major axis is parallel to the propagation direction of the laser beam for an orientation of $\theta = 0°$. For radius $r_2$, which is perpendicular to the optical axis, the reference radius $r_{\mathrm{Ref}}$ is divided by the same elongation factors to maintain a constant area for all the particles. The classical mathematical sign convention is used throughout the text (e.g., a positive angle $\theta$ indicates a counterclockwise rotation of the particle). In the same way, a positive torque will cause a rotational acceleration of the particle in the counterclockwise direc-

tion; a negative torque will cause a clockwise rotational acceleration of the particle. The refractive index was chosen to be 1.5 for the particles, and they are embedded in air.

In Section 3 we will first present the size-dependent torque for a rotation angle of the particles of 45° to give an overall indication about the evolution of the torque. Subsequently we will discuss in detail the characteristics of the torque at different sizes. We analyze the difference in the behavior for particles with a size much smaller than the wavelength, intermediate sizes, and particles with a size comparable to the wavelength.

## 3. NUMERICAL RESULTS AND DISCUSSION

### A. Size Dependence

In Fig. 1(a) the torque on an elliptical cylinder for the three different elongations as a function of $r_{\mathrm{Ref}}$ is shown. The rotation angle $\theta$ is 45° and we have assumed a TE-polarized beam for the illumination. The inset shows the particle orientation with respect to the propagation direction of the illuminating wave field. The particle is positioned at the center of the beam waist ($x = 0, z = 0$). The results for the same configuration but with a TM-polarized beam are shown in Fig. 1(b).

The torque for TE polarization has a positive sign for very small particles, which will cause an alignment of the minor axis parallel to the propagation direction of the beam. Increasing the size will cause a steady increase in the induced torque up to a particle radius of $r_{\mathrm{Ref}} \approx 0.25\lambda$. For the two most elongated particles, increasing the size will cause a decrease in the strength of the torque. For these two particles this leads ultimately to a reversal of the torque direction. The torque exerted on the particle with an elongation factor of $\sqrt{2}$ continues on an upward trend. For a further increase of the size, the torque will increase again for all three particles, leading again to a change of sign for the two most elongated particles. As will be shown in Subsection 3(b), an exact designation of the alignment direction for these larger particle sizes is not possible, because different rotation angles exist for which the net torque becomes zero.

For TM polarization, the overall behavior is comparable, except for a change in the sign of the torque. For particles much smaller than the wavelength, the torque is negative, which will cause an alignment of the particle with the major axis parallel to the propagation direction of the illuminating wave field. This is the orientation that one would expect from a simple dipole model. When we increase the size of the particles slightly, the torque

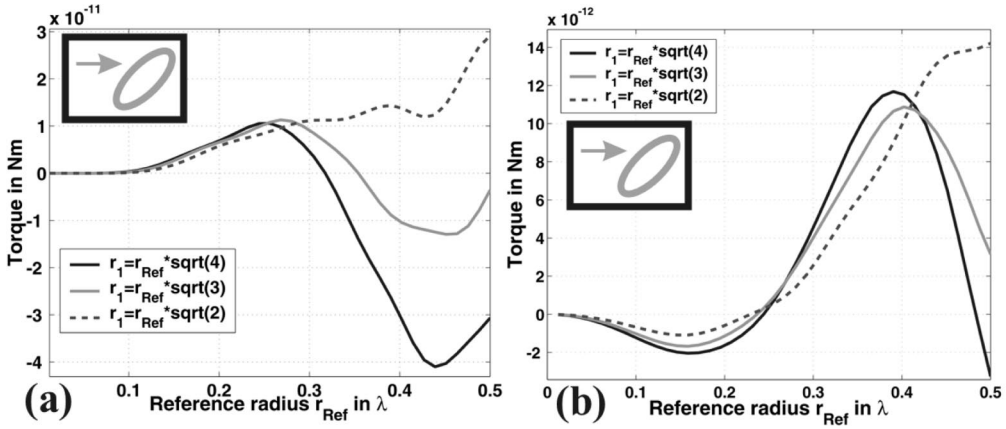


Fig. 1. Torque on elliptical cylinders located at the center of the beam waist oriented at 45° for (a) TE polarization and (b) TM polarization as a function of the size.

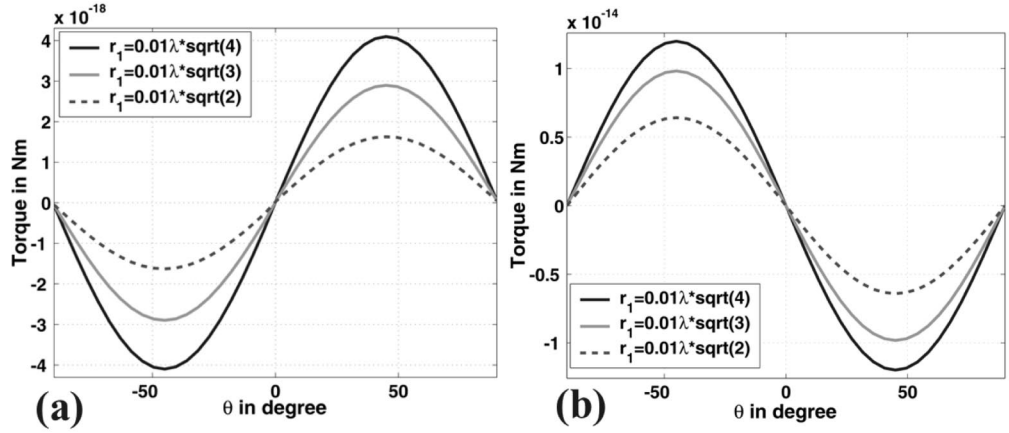


Fig. 2. Torque on elliptical cylinders much smaller than the wavelength ($r_1 = 0.01\lambda$) as a function of the orientation for (a) TE polarization and (b) TM polarization.

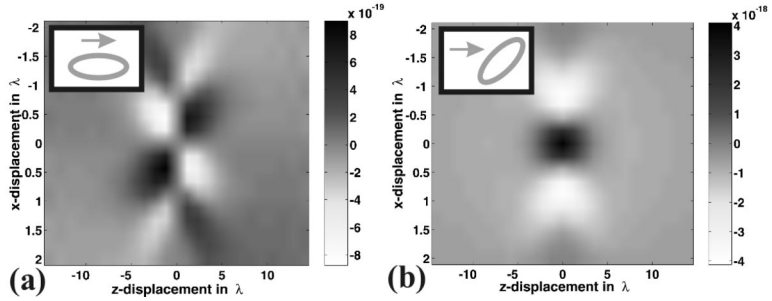


Fig. 3. Spatial distribution of the torque for an elliptical cylinder much smaller than the wavelength ($r_1 = 0.01\lambda\sqrt{4}$) oriented at (a) $\theta = 0°$ and (b) $\theta = 45°$ for TE polarization.

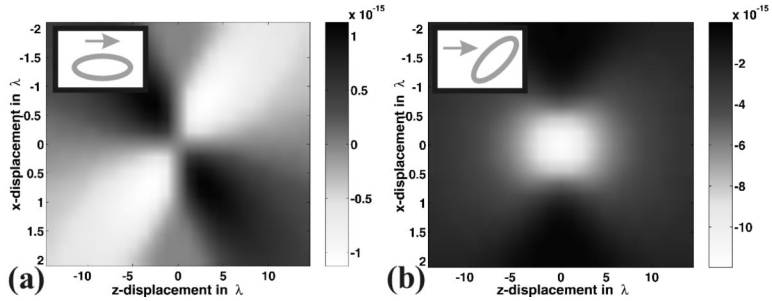


Fig. 4. Spatial distribution of the torque for an elliptical cylinder much smaller than the wavelength ($r_1 = 0.01\lambda\sqrt{4}$) oriented at (a) $\theta = 0°$ and (b) $\theta = 45°$ for TM polarization.

becomes larger in magnitude with the same size, independent of the elongation. At a certain size of the particle, the strength of the torque becomes lower and a change of sign occurs at a size of $r_{\mathrm{Ref}} \approx 0.25\lambda$. A further increase in the particle size will first cause an increase of the torque, and then from a certain particle size the torque diminishes. The maximum of the torque for the two most elongated particles is at approximately a radius of $r_{\mathrm{Ref}} = 0.4\lambda$. The change in the sign of the torque is attributed to the change in the polarization direction, as the electric field component has a dominant influence on the torque. For TE polarization the electric field will oscillate parallel to the cylinder axis and will have no component in the plane of rotation, such that it does not contribute to the torque in the dipole approximation.

In Subsections 3(b)–3(d) the torque for different size domains is analyzed as a function of the orientation as well as the spatial position of the particle within the illuminating wave field. In each of these domains the resulting torque shows different characteristic features. The size domains to be investigated are particles much smaller than the wavelength, particles with a size comparable to the wavelength, and particles with a size between the two (called the intermediate region).

### B. Particles Much Smaller than the Wavelength

The influence of the electric field can be seen when we compare the strength of the torque exerted on the particles for the two linear polarizations, if the particles are very small compared to the wavelength. In this size domain the scattered field of the particle is basically given by the field of a dipole. In Fig. 2(a) for the TE polarization and in Fig. 2(b) for the TM polarization the torque on differently elongated particles as a function of the rotation angle $\theta$ is shown. The radius for the particles is $r_{\mathrm{Ref}} = 0.01\lambda$. The torque shows a sinusoidal dependence on the angle between the optical axis and the major axis of the particle. The strength of the torque for the TE polarization is smaller by four orders of magnitude.

In contrast, the forces applied on the particles by the illuminating wave field are slightly higher for the TE- than for TM-polarized light.[26] By using rigorous diffraction theory or the dipole approximation, we can show that for TE polarization the force will not depend on the particle elongation or the particle orientation in the quasi-static approximation.[26] The polarizability of the particles is independent of the axis ratio. Consequently the torque becomes zero because the particle behaves effectively like a circular cylinder, whose torque is always zero at the center of the waist. The remaining nonzero torque, even for very small particles, is the result of the rigorous solution of the problem, which takes higher multipoles and the influence of the magnetic field fully into account. With TE polarization the torque is smaller by four orders of magnitude compared with the torque exerted on geometrically identical particles with TM-polarized light. Hence the torque can be regarded as effectively equal to zero. For a pure electric dipole, the polarization vector and the electric field vector will have the same direction, such that the torque, defined as $\tau = \mathbf{p}\times\mathbf{E}$, is zero.

The dependence on the rotation angle for both polarizations is nearly perfectly sinusoidal. The spatial distribution can be seen in Fig. 3(a) at $\theta = 0°$ and in Fig. 3(b) at $\theta = 45°$ for TE polarization. The torque is shown as a function of the displacement of the particle from the waist of the laser beam. The illuminating beam propagates in the positive $z$ direction, meaning from the left to the right side of the figure. For the TE polarization, a significant

nonzero torque is concentrated only around the region of the waist. If the orientation of the particle is with the major axis parallel to the optical axis ($\theta = 0°$), a change of sign appears for positions of the particle behind the waist as well as for positions on the different sides of the optical axis. When the particle is rotated, the force distributions before and after the waist adopt a similar form. At an orientation of 45°, the distribution is nearly symmetric with respect to the waist of the laser.

In Fig. 4(a) at a particle orientation $\theta = 0°$ and in Fig. 4(b) at $\theta = 45°$, the same force distributions are shown assuming TM polarization. The basic behavior, like the change of sign in the torque along the different axes at $\theta = 0°$, is the same as for the TE polarization, but the strength is much higher. The torque distribution for a particle rotation of 45° is proportional to the square of the amplitude of the illuminating Gaussian beam.

The qualitative force distributions for the different elongated particles will not depend on the axis ratio, but the strength of the torque will scale with the axis ratio of the particle. The strength and the axis ratio have the same ratio everywhere in space. For an increase in the particle size, the sinusoidal dependence of the torque will be reduced and the distribution becomes slightly asymmetric. Figure 5(a) for TE polarization and Fig. 5(b) for TM polarization show the torque in the center of the waist for the three axis ratios as a function of the rotation angle. The radius of the particles is $r_{\mathrm{Ref}} = 0.1\lambda$. The strength of the torque for TE-polarized light is still smaller but now only by a single order of magnitude. The sinusoid is somewhat stretched toward the larger rotation angle, and the maximum of the torque is now at approximately $\pm 50°$ for both polarizations. The difference in the sign of the torque still exists.

Overall the torque in this size domain shows a sinusoidal dependence on the angle between the particle and the optical axis. For smaller particles, which more closely satisfy the dipole approximation, the response is closer to a sinusoid. For a slightly increased size, the maximum of the torque is shifted to slightly larger angles and the response becomes asymmetric.

### C. Particles with an Intermediate Size

With a further increase in the particle size, the dipole approximation is no longer valid and effects can be observed that can be explained only by taking into account multiple reflections of the light inside the particles. These intermediate-sized particles will be analyzed in this subsection.

In this size domain the asymmetry of the torque on the orientation increases but the maximum of the torque tends to smaller rotation angles. This is shown in Fig. 6 for particles with a radius of $r_{\mathrm{Ref}} = 0.3\lambda$ with TE polarization. The orientation for which the particle can be held at a stable rotational position now deviates from 90°. In this case, the angles for which the particle is held stable are between 50° and 60°. As the orientation of $\theta = 90°$ indicates an alignment with the minor axis parallel to the propagation direction of the beam, the smaller angle corresponds to an orientation with a certain deviation from this cardinal direction. Additional points with a net torque of zero exist, but these points are unstable. This behavior can only be explained by the complicated diffraction process, in which multiple reflections inside the particle appear. As the radius of the particle is now approximately a quarter of the wavelength, the reflections will accumulate a phase delay close to $\pi$, such that constructive and destructive interference will play a dominant role. A similar behavior can be observed for TM polarization.

The size of the particle for which the sign of the torque inverts at a rotation angle of 45° is smaller for TM than for TE polarization. An additional difference is the orientation at which the particle can be held stable. For TM polarization, the particle is stably trapped along the minor as well as the major axis of the elliptical particle. A third orientation between these two also has a net torque equal to zero, but the point is unstable. For TE polarization, it is the opposite: The particle is held stable at this intermediate position and the particle is unstable for the orientations along the two principal axes.

In addition, for TM polarization, despite the change of sign, the resulting torque as a function of the orientational angle for a slightly increased particle size will show a smooth and close to sinusoidal dependency. This can be seen in Fig. 7. The particle has a radius of $r_{\mathrm{Ref}} = 0.3\lambda$. Now there will be only a single orientation for which the particle is stable, with the minor axis parallel to the propagation direction of the illumination. The entire

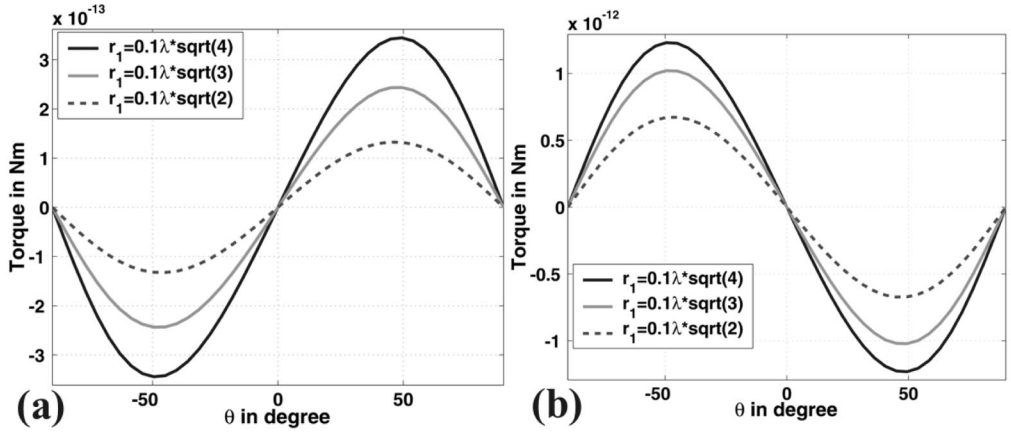


Fig. 5. Torque on elliptical cylinders smaller than wavelength ($r_{\mathrm{Ref}} = 0.1\lambda$) as a function of the orientation for (a) TE polarization and (b) TM polarization.

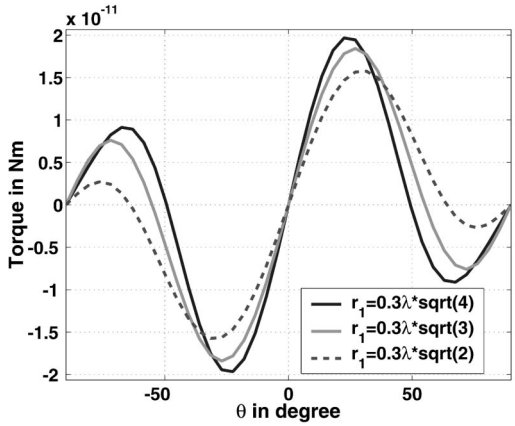


Fig. 6. Torque on elliptical cylinders of an intermediate size ($r_{\mathrm{Ref}} = 0.3\lambda$) as a function of the orientation for TE polarization.

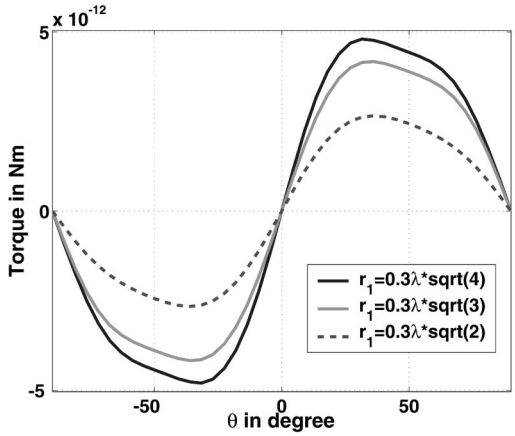


Fig. 7. Torque on elliptical cylinders of an intermediate size ($r_{\mathrm{Ref}} = 0.3\lambda$) as a function of the orientation for TM polarization.

spatial torque distribution will suffer from this change in the sign. Figure 8(a) shows the torque as a function of the displacement of the particle at a rotation angle of 0°, and Fig. 8(b) shows the torque for a particle oriented at 45°. In the distribution for the torque on the particle oriented at 0°, the torque is maximum at positions somewhat after the waist. A significant asymmetry in the torque for the particle oriented at 45° can be seen, which is due to the comparable size of the particle and the beam waist.

Summarizing the results of this subsection, we can state that, for intermediate-sized particles, the angle-dependent torque becomes more asymmetric. In TM polarization the particles are stably trapped along the major axis as well as along the minor axis. A third point exists with a zero net torque but the point is unstable. For TE polarization it is the opposite case, as the particle is stably trapped at this angle and unstable along the major and minor axis.

### D. Particles with a Large Size

For a further increase in the particle size with a radius significantly above a third of a wavelength, the response becomes more complex and different orientations exist for which the particles are rotationally stable.

For this size regime, a simple relation between the torque and the particle geometry is not possible. Figure 9(a) shows the torque at the center of the waist for particles with a radius of $r_{\mathrm{Ref}} = 0.5\lambda$ for TE polarization, and Fig. 9(b) shows the torque for TM polarization. It can be seen that for some of the particles, different orientations exist at which the particle is stable and the net torque is zero. For TE polarization, the particle with a radius of $r_1 = 0.5\lambda\sqrt{3}$ can be held at an angle $\theta$ of $\pm 71°$ and $\pm 28°$. The strength of the torque for the two polarizations is comparable and is even slightly larger for TE-polarized light.

Nevertheless, the spatial distribution of the torque will show similarities for all the particles. The distributions for the two particles oriented at $\theta = 0°$ and $\theta = 45°$ are shown for TE polarization in Figs. 10(a) and 10(b). The spatial distribution for the same particle but illuminated with TM-polarized light is qualitatively the same as for TE polarization. They differ only slightly in strength. For the particle aligned with the major axis parallel to the optical axis, the torque above the optical axis ($x > 0$) is always negative and below the axis it is positive for the two polarizations. The particles oriented at 45° will exhibit a maximum torque for a position above the optical axis. The torque is nearly zero at positions below the optical axis.

## 4. CONCLUSION

In this paper we have analyzed the torque exerted on dielectric elliptical cylinders by a highly focused Gaussian beam. Basically three different size domains have been identified, which show various characteristics in their torque response as a function of the orientation of the particle with respect to the illuminating beam as well as in their spatial behavior with respect to position within the wave field.

It was found that for particles much smaller than the wavelength, the torque depends perfectly sinusoidally on the angle between the particle orientation and the illumination direction of the laser beam. The torque will cause an orientation for the TM polarization of the major axis parallel to the optical axis and for the TE polarization with the minor axis parallel to the optical axis. Increasing the size causes deviations of the angle-dependent torque from the sinusoidal angle dependency, and an additional orientation exists at which the torque is zero. For TM polarization this is an unstable orientation. In TE polarization this orientation is the only stable orientation, and for an orientation along the minor axis or the major axis the torque is zero but the orientations are unstable. For a further increase of the size, various orientations exist for which the particle is rotationally stable. The overall orientational dependence of the torque shows a complex pattern. Such a behavior can be analyzed only by use of rigorous diffraction theory.

The strength of the torque for particles much smaller than the wavelength is significantly smaller for TE than for TM polarization. We have attributed this significant difference to the dominant influence of the electric field component, which oscillates for TE polarization parallel to the infinite cylinder axis. In TM polarization the elec-

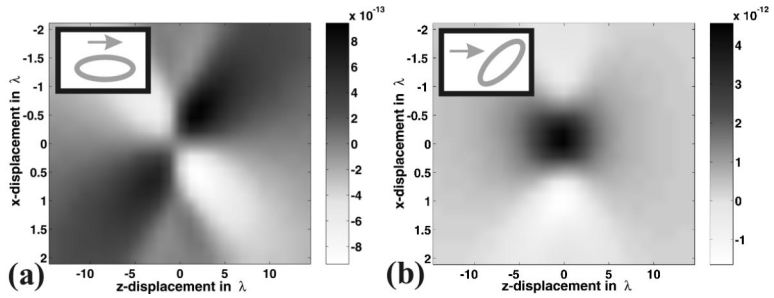


Fig. 8. Spatial distribution of the torque for an elliptical cylinder of an intermediate size ($r_1 = 0.3\lambda\sqrt{4}$) oriented at (a) $\theta = 0°$ and (b) $\theta = 45°$ for TM polarization.

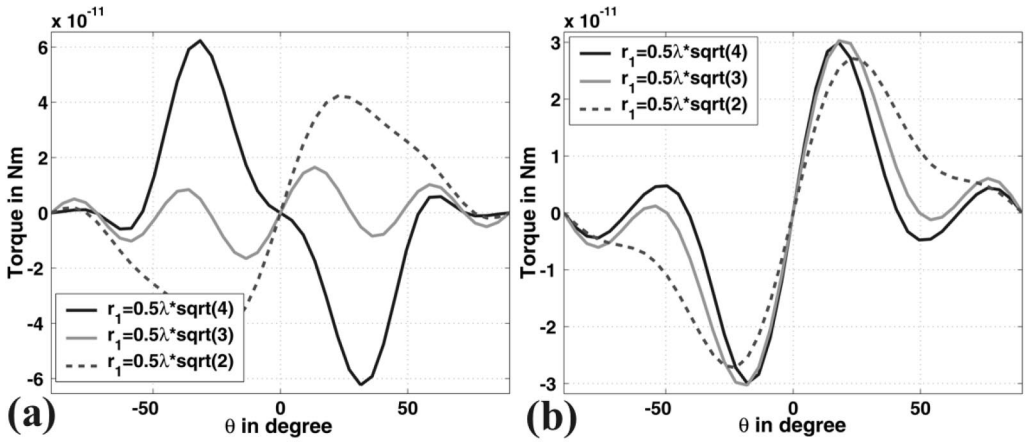


Fig. 9. Torque on elliptical cylinders of a size comparable to the wavelength ($r_{\mathrm{Ref}} = 0.5\lambda$) as a function of the orientation for (a) TE polarization and (b) TM polarization.

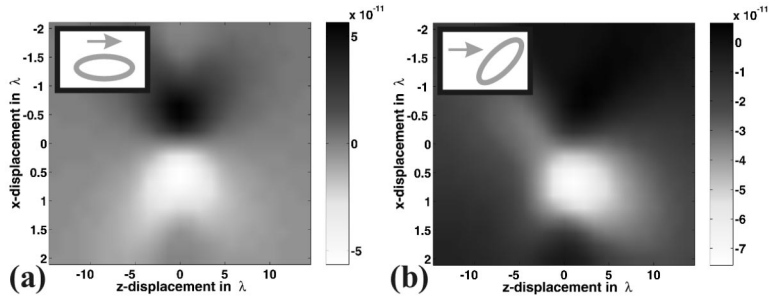


Fig. 10. Spatial distribution of the torque for an elliptical cylinder of a size comparable to the wavelength ($r_1 = 0.5\lambda\sqrt{4}$) oriented at (a) $\theta = 0°$ and (b) $\theta = 45°$ for TE polarization.

tric field oscillates perpendicular to the cylindrical axis and will cause a strong rotational acceleration of the particle. For particles with a size comparable to the wavelength, the strength of the torque is comparable for the two polarizations.

The possibility of self-alignment of particles upon illumination offers an interesting application for the precise writing of nano-optical devices that make use of elliptical particles. One example could be a plasmonic waveguide made of metallic nanoparticles. Because the wavelength for which a surface plasmon is excited in the particle depends strongly on the geometry, waveguides with different operating wavelengths could be fabricated by using particles with the appropriate shape. To create the waveguide, that is, a chain of particles, optical tweezers could be used. The particles are aligned by choosing the proper illumination parameters. With a parallelized optical tweezer generated, e.g., by a diffractive fan-out element or just by a standing pattern of plane waves propagating in different directions, it would be possible to write photonic crystals based on elliptical particles with high precision, because the particles trapped at the appropriate periodic points will be aligned to form a perfect symmetric pattern in all directions.

Another field of research that has promising applications and is currently under investigation is the self-alignment of particles by interaction with neighboring objects. In a system, e.g., proposed by Li *et al.*,[27] a chain of metallic particles with descending size is used as a novel type of plasmonic lens that concentrates an extremely large amount of energy into a small spatial region to yield a highly confined light source. With an appropriate illu-

minating field, the particles could attract as well as orient each other in such a way that the efficiency of the proposed nanolens is maximized.

## ACKNOWLEDGMENT

This research was supported by the European Union within the framework of the Future and Emerging Technologies program Super Laser Array Memory under grant IST-2000-26479.

Carsten Rockstuhl can be reached by e-mail at carsten.rockstuhl@unine.ch.

## REFERENCES

1. A. Ashkin, "Acceleration and trapping of particles by radiation pressure," Phys. Rev. Lett. **24**, 156–159 (1970).
2. A. Ashkin and J. M. Dziedzic, "Optical levitation by radiation pressure," Appl. Phys. Lett. **19**, 283–285 (1971).
3. D. G. Grier, "A revolution in optical manipulation," Nature (London) **424**, 810–816 (2003).
4. A. Ashkin, "Optical trapping and manipulation of neutral particles using lasers," Proc. Natl. Acad. Sci. USA **94**, 4853–4860 (1997).
5. R. C. Gauthier and A. Frangioudakis, "Theoretical investigation of the optical trapping properties of a micro-cubic glass structure," Appl. Opt. **39**, 3060–3070 (2000).
6. Y. Harada and T. Asakura, "Radiation forces on a dielectric particle in the Rayleigh scattering regime," Opt. Commun. **124**, 529–541 (1996).
7. S. Kawata, Y. Inouye, and T. Sugiura, "Near-field scanning optical microscope with a laser trapped particle," Jpn. J. Appl. Phys., Part 1 **33**, L1725–L1727 (1994).
8. A. Rohrbach, E. L. Florin, and E. H. K. Stelzer, "Photonic force microscopy: simulation of principles and applications," in *Photon Migration, Optical Coherence Tomography, and Microscopy*, S. Andersson-Engels and M. F. Kaschke, eds., Proc. SPIE **4431**, 75–86 (2001).
9. P. L. Marston and J. H. Crichton, "Radiation torque on a sphere caused by a circularly-polarized electromagnetic wave," Phys. Rev. A **30**, 2508–2516 (1984).
10. A. T. O'Neil and M. J. Padgett, "Three-dimensional optical confinement of micron-sized metal particles and the decoupling of the spin and orbital angular momentum with an optical spanner," Opt. Commun. **185**, 139–143 (2000).
11. M. E. J. Friese, T. A. Nieminen, N. R. Heckenberg, and H. Rubinsztein-Dunlop, "Optical torque controlled by elliptical polarization," Opt. Lett. **23**, 1–3 (1998).
12. S. Bayoudh, T. A. Nieminen, N. R. Heckenberg, and H. Rubinsztein-Dunlop, "Orientation of biological cells using plane-polarized Gaussian beam optical tweezers," J. Mod. Opt. **50**, 1581–1590 (2003).
13. A. I. Bishop, T. A. Nieminen, N. R. Heckenberg, and H. Rubinsztein-Dunlop, "Optical application and measurement of torque on microparticles of isotropic nonabsorbing material," Phys. Rev. A **68**, 033802 (2003).
14. P. Galadja and P. Ormos, "Orientation of flat particles in optical tweezers by linearly polarized light," Opt. Express **11**, 446–451 (2003), http://www.opticsexpress.org.
15. P. Galajda and P. Ormos, "Complex micromachines produced and driven by light," Appl. Phys. Lett. **78**, 249–251 (2001).
16. M. E. J. Friese, H. Rubinsztein-Dunlop, J. Gold, P. Hagberg, and D. Hanstorp, "Optically driven micromachine elements," Appl. Phys. Lett. **78**, 547–549 (2001).
17. T. A. Nieminen, N. R. Heckenberg, and H. Rubinsztein-Dunlop, "Optical measurement of microscopic torques," J. Mod. Opt. **48**, 405–413 (2001).
18. H. Polaert, G. Gréhan, and G. Gousbet, "Forces and torques exerted on a multilayered spherical particle by a focused Gaussian beam," Opt. Commun. **155**, 169–179 (1998).
19. J. P. Barton, D. R. Alexander, and S. A. Schaub, "Theoretical determination of net radiation force and torque for a spherical particle illuminated by a focused laser beam," J. Appl. Phys. **66**, 4594–4602 (1989).
20. T. A. Nieminen, H. Rubinsztein-Dunlop, N. R. Heckenberg, and A. I. Bishop, "Numerical modelling of optical trapping," Comput. Phys. Commun. **142**, 468–471 (2001).
21. C. Hafner, *Post-Modern Electromagnetics* (Wiley, New York, 1999).
22. L. Novotny, R. X. Bian, and X. S. Xie, "Theory of nanometric optical tweezers," Phys. Rev. Lett. **79**, 645–648 (1997).
23. C. Hafner, *The Generalized Multipole Technique for Computational Electromagnetics* (Artech House, Norwood, Mass., 1990).
24. X. Wang, X.-B. Wang, and P. R. C. Cascoyne, "General expressions for dielectrophoretic force and electrostational torque derived using the Maxwell stress tensor," J. Opt. Commun. **39**, 277–295 (1997).
25. M. Lester and M. Nieto-Vesperinas, "Optical forces on microparticles in an evanescent laser field," Opt. Lett. **24**, 936–938 (1999).
26. C. Rockstuhl and H. P. Herzig, "Rigorous diffraction theory applied to the analysis of the optical force on elliptical nano- and micro-cylinders," J. Opt. A Pure Appl. Opt. **6**, 921–931 (2004).
27. K. Li, M. I. Stockman, and D. J. Bergman, "Self-similar chain of metal nanospheres as an efficient nanolens," Phys. Rev. Lett. **91**, 227402 (2003).